frontiers | Frontiers in Food Science and Technology

TYPE Original Research
PUBLISHED 22 August 2024
DOI 10.3389/frfst.2024.1444298

OPEN ACCESS

EDITED BY
Miguel Rebollo-Hernanz,
Autonomous University of Madrid, Spain

REVIEWED BY
Jun Liu,
Yangzhou University, China
Rungsinee Sothornvit,
Kasetsart University, Thailand

*CORRESPONDENCE
Sawsan Affes,
sawsanaffes170@gmail.com

RECEIVED 05 June 2024
ACCEPTED 07 August 2024
PUBLISHED 22 August 2024

CITATION
Affes S, Aranaz I, Acosta N, Heras Á, Nasri M and Maalej H (2024) Silver nanoparticles incorporated with enzymatically derived chitooligosaccharides: preparation, characterization, and biological potential evaluation.
Front. Food. Sci. Technol. 4:1444298.
doi: 10.3389/frfst.2024.1444298

Silver nanoparticles incorporated with enzymatically derived chitooligosaccharides: preparation, characterization, and biological potential evaluation

Sawsan Affes[1]*, Inmaculada Aranaz[2], Niuris Acosta[2], Ángeles Heras[2], Moncef Nasri[1] and Hana Maalej[3]

[1]Laboratory of Enzyme Engineering and Microbiology, National School of Engineering of Sfax (ENIS), University of Sfax, Sfax, Tunisia, [2]Department of Chemistry in Pharmaceutical Science, Faculty of Pharmacy. Pluridisciplinar Institute, Complutense University of Madrid, Madrid, Spain, [3]Laboratory of Biodiversity and Valorization of Arid Areas Bioresources (BVBAA), LR16ES36, Faculty of Sciences of Gabes, University of Gabes, Gabes, Tunisia

In this work, silver nanoparticles (AgNPs) were elaborated using a simple, low-cost, and reproducible method by thermal treatment at 90°C of chitooligosaccharides (COSs), produced by chitosan depolymerization using the digestives chitosanases from *Portunus segnis* viscera, in the presence of $AgNO_3$. The characterization of the obtained AgNPs, using UV–visible spectroscopy, transmission electron microscopy (TEM), dynamic light scattering (DLS), and Fourier-transform infrared (FTIR) spectroscopy analyses, showed that they are crystalline, spherical and stable for a month at 4°C. Moreover, the biological properties of the synthesized AgNPs were evaluated, proving that they exhibited interesting antioxidant and antibacterial activities. The present investigation suggested that COSs will be a good source for the preparation of AgNPs that could be useful in different industrial and biomedical applications.

KEYWORDS

chitooligosaccharides, bioactive silver nanoparticles, physicochemical properties, antioxidant activity, antibacterial activity

1 Introduction

Currently, silver nanoparticles (AgNPs) are of particular interest due to their potential applications in various fields, especially in pharmacological, biomedical, and food industries, due to their low toxicity, high stability, and unique optical, mechanical, catalytic, and biological properties (Dara et al., 2020; Wu et al., 2021; Yang et al., 2022; Mohan et al., 2024). Different methods of AgNP production are used, including chemical, physical, and biological processes (Hajji et al., 2017; Pirtarighat et al., 2018; Dara et al., 2020; Dong et al., 2022). Among these techniques, the biological synthesis of silver nanoparticles is a green, ecofriendly method that produces stable and soluble AgNPs with a high yield, mainly using natural biopolymers, such as cellulose, collagen, and chitosan (Novaes et al., 2020; Wu et al., 2021; Tang et al., 2023; Mohan et al., 2024). Noble silver nanostructures encapsulated within or on biopolymers are of particular interest in many applications as they combine the physicochemical features of noble metal structures and the biological features of polymers (Zienkiewicz-Strzałka et al., 2020; Dong et al., 2022; Santiago-Castillo et al., 2022).

Due to its interesting biological properties, such as biocompatibility, non-toxicity, biodegradability, and antimicrobial and antioxidant activities, as well as its ability to produce and stabilize silver nanoparticles, chitosan is one of the most exploited biopolymers, derived from chitin and extracted from the exoskeleton of crustaceans by deacetylation (Affes et al., 2020 b; Herrera et al., 2018; Muddin et al., 2024; Zienkiewicz-Strzałka et al., 2020). The basic structure of this natural polysaccharide is the sequence of repeated β (1–4)-linked N-acetyl-D-glucosamine and D-glucosamine units with one amino group (NH_2) and two hydroxyl groups (OH) (Dara et al., 2020; Affes et al., 2021). Recently, owing to their lower viscosity and greater solubility, mainly due to their shorter chain lengths, as well as better antimicrobial and antioxidant properties, low-molecular-weight (Mw) chitosan derivatives or chitooligosaccharides (COSs), produced by chitosan modification using chemical, physical, or enzymatic methods, have attracted more interest than chitosan (Affes et al., 2020a; Affes et al., 2022a; Affes et al., 2022b; Chen et al., 2022).

The COS structure contains unique functional groups that play an important role in their interactions with metal ions and metal nanoparticles. Indeed, the primary amino groups of chitosan and chitooligosaccharides interact with metal surfaces and also act as capping sites for nanoparticle stabilization (Aranaz et al., 2018; Zienkiewicz-Strzałka et al., 2020; Muddin et al., 2024). Furthermore, the addition of chitosan and its derivatives in nanoparticle production enhances the overall biocompatibility and non-toxicity of the elaborated composite that will be suitable for use in biomedical and environmental applications (Muddin et al., 2024).

Moreover, the synthesis of nanoparticles using eco-friendly "greener" methods is important to consider, especially when using biomaterials extracted from renewable sources, such as several natural polymers, including dextrose, arabinose, starch, polyvinyl alcohol, and chitosan and its derivatives (Hajji et al., 2017). In addition, it has been reported that COS samples have a great ability to reduce and stabilize AgNPs (Aranaz et al., 2018; Tang et al., 2023), and they have been used as an alternative to high-Mw chitosan because of their similar biochemical properties but higher water solubility and biological activities, including antimicrobial and antioxidant properties (Tang et al., 2023). Indeed, the smaller Mw of COS also facilitates a better ability to penetrate bacterial cells and interfere with the transcription of DNA.

In this context, an attempt was made to elaborate an effective process for the synthesis of chitosan and COS-based AgNPs with amplified biological properties. The physicochemical characterization of the produced AgNPs was carried out using UV–visible spectroscopy, transmission electron microscopy (TEM), dynamic light scattering (DLS), and Fourier-transform infrared (FTIR) spectroscopy analyses. Their antibacterial and antioxidant activity was further studied.

2 Materials and methods

2.1 Production and physicochemical characterization of chitosan and COSs

Chitosan (C1: Mw = 1,244.70 kDa; acetylation degree (AD) = 7.60 ± 0.54%) used in this work was prepared by the deacetylation of shrimp shell chitin, as mentioned in our previous study (Affes et al., 2019). COSs were prepared by the enzymatic depolymerization of chitosan using the digestive acid chitosanase extracted from blue crab *Portunus segnis* viscera (Affes et al., 2019). In brief, chitosan (1% (w/v), dissolved in acetic acid (1 M; pH 4.0) was incubated in a thermostatic water bath at 40°C with *P. segnis* chitosanolytic preparation (ratio E/S = 100 U/g chitosan). Samples were withdrawn at 1 and 24 h, then heated at 100°C for 10 min, neutralized to pH 8.0, and finally centrifuged at 8,000 ×g for 30 min. The insoluble parts obtained at 1 and 24 h were referred to as COS (C2 and C3), respectively. COSs were freeze-dried, and white powders were recovered.

The average Mw and AD of the prepared COSs were determined by SEC-HPLC and the first derivative UV–spectrophotometric method, respectively.

2.2 Elaboration and characterization of silver nanoparticles

Colloidal AgNPs were prepared using chitosan (C1) and COS (C2 and C3) as reducing and stabilizing agents, respectively. Chitosan (1% w/v) was dissolved in acetic acid (0.1 M), whereas COSs (C2 and C3) (1% w/v) were dissolved in ultrapure water, followed by stirring for 24 h. For AgNP production, 200 µL of freshly prepared silver nitrate ($AgNO_3$ > 99%) (5 mM), dissolved in water, was added to 1 mL of each polymeric solution. The resulting mixtures were thermally treated at 90°C at different incubation times (1, 2, 3, 4, and 24 h) in a closed container to avoid solvent evaporation. Colloidal nanoparticles, referred to as AgNPs-C1, AgNPs-C2, and AgNPs-C3, were stored under dark conditions at 4°C until further study. For the preparation of scaffolds, the produced AgNPs were freeze-dried.

The produced AgNPs were characterized using UV–visible spectroscopy, transmission electron microscopy (TEM), and dynamic light scattering analysis.

2.3 Biological activity evaluation

2.3.1 Antioxidant activity

2.3.1.1 DPPH and ABTS radical-scavenging potentials

The ability of AgNPs to scavenge 1,1-diphenyl-2-picrylhydrazyl (DPPH) radical was determined according to the method proposed by Bersuder et al. (1998).

The capacity of AgNPs to quench the long-lived 2,2′-azino-bis (3-ethylbenzothiazoline-6-sulfonic acid) ($ABTS^+$) species was also studied according to the method proposed byRe et al. (1999). Butylated hydroxyl-anisole (BHA) was used as a positive control at 1%.

2.3.1.2 Reducing power assay

The ability of BHA and AgNPs to reduce iron (III) was determined according to the method described by Yildirim et al. (2001). Higher absorbance of the reaction mixture showed higher reducing power. The experiments were carried out in triplicate.

TABLE 1 Average molecular weight (Mw, kDa) and acetylation degree (AD, %) of chitosan (C1) and chitooligosaccharides (COSs: C2 and C3).

Polymer	Abbreviation	Mw (kDa)	AD (%)
Chitosan	C1	1244.70	7.60 ± 0.54^{B}
$COS_{1\ h}$	C2	<4.4	18.71 ± 0.09^{A}
$COS_{24\ h}$	C3	<4.4	18.20 ± 1.19^{A}

Values are the mean ± standard deviation (n = 3). Means with different letters (A–B) and within a column indicate significant difference ($p < 0.05$).

2.3.1.3 Total antioxidant activity

The total antioxidant activity of BHA and AgNPs to reduce Mo (VI) to Mo (V) and to form a green phosphate/Mo (V) complex at acidic pH was tested, as reported by Prieto et al. (1999). The total antioxidant activity was expressed as α-tocopherol equivalents (μmol/mL).

2.3.2 Antibacterial activity

The antibacterial activity assay of the prepared AgNPs was performed according to the agar diffusion method described by Vanden Berghe and Vlietinck (1991). Three Gram-negative bacteria, *Salmonella enterica*, *Pseudomonas aeruginosa*, and *Enterobacter* spp., and four Gram-positive strains, *Staphylococcus aureus*, *Micrococcus luteus*, *Listeria monocytogenes*, and *Bacillus cereus*, were tested. First, culture suspension of the tested strains was spread over the Mueller–Hinton agar medium. Then, 60 μL of each solution was added to the wells, previously cut in the agar. The antibacterial activity was detected after incubation at 37°C for 24 h and determined by measuring the diameter of the growth inhibition zone around the wells (including a well diameter of 6 mm).

2.4 Statistical analysis

All experiments were carried out in triplicate, and average values with standard deviation (n = 3) were reported. Mean separation and significance were analyzed using the SPSS software package v17.0 professional edition (SPSS, Inc., Chicago, IL, United States) using ANOVA. Differences were considered significant at $p < 0.05$.

3 Results and discussion

3.1 Preparation and characterization of AgNPs

In this work, chitosan (C1) (Mw = 1,244.7 kDa; AD = 7.6%) and low-molecular-weight COSs (Mw < 4.4 kDa, AD around 18%), C2 and C3, obtained by the enzymatic hydrolysis of chitosan using the digestive acid chitosanases from *P. segnis* crab after 1 and 24 h, respectively, were studied in terms of their ability to produce and stabilize AgNPs (Table 1).

To this end, chitosan and COS solutions containing $AgNO_3$ were thermally treated at 90°C. As shown in Figure 1A, a change in the color of chitosan/$AgNO_3$ mixtures was visualized from colorless at T = 0 h to yellow at T = 2 h and then to brown at T = 24 h. For COS/$AgNO_3$ mixtures, brown solutions were obtained at 2 h, and treatment for 24 h led to their aggregation. The color changes indicate the formation of AgNPs by the coordination between Ag^+ and NH_2 functions of chitosan and their derivatives, followed by reduction by thermal treatment (Aranaz et al., 2018; Dara et al., 2020).

The biosynthesis and stability of AgNPs were further highlighted by UV–vis spectroscopy based on the characteristic surface plasmon resonance (SPR) peak observed at approximately 400–450 nm, confirming the AgNP formation by the interaction between the amino and hydroxyl groups of chitosan and its derivatives with silver ions (Figure 1B). AgNPs-C1, obtained after heating during 24 h, showed broad spectra with higher maximum absorbance (438 nm) than those of AgNPs-C2 and AgNPs-C3, obtained after 2 h (436 and 427 nm, respectively), suggesting a broad AgNP distribution using chitosan and lower-sized and less polydispersed AgNPs using COS (Aranaz et al., 2018, Dara et al., 2020; Mohan et al., 2024; Santiago-Castillo et al., 2022) Dara et al. (2020) observed that chitosan–AgNPs prepared by thermal treatment in the presence of NaOH showed lower maximum absorbance at 419 nm, stating that the concentration of silver salt, the morphological shape, size, and distribution of AgNPs, and the addition of NaOH for the growth of AgNPs influence the intensity of the SPR band and the absorbance of AgNPs. Reicha et al. (2012) showed surface plasmon absorption at approximately 420 nm for chitosan–silver nanoparticles prepared by an electrochemical oxidation/complexation process, followed by UV irradiation reduction.

Furthermore, these same maximum wavelengths of AgNPs-C1 (24 h) and AgNPs-C2 and C3 (2 h) remained stable during storage for 1 month at 4°C (Figure 1C), demonstrating the ability of chitosan and its derivatives to stabilize the elaborated AgNPs and prevent their aggregation (Kalaivani et al., 2018; Dara et al., 2020).

The characterization of the produced AgNPs, AgNPs-C1 (24 h), AgNPs-C2 (2 h), and AgNPs-C3 (2 h) was then carried out. TEM analysis was used to visualize the crystalline nature, morphology, and size of the produced NPs (Figure 2). TEM micrographs showed the polycrystalline (Figure 2A), dispersed, and spherical form of NPs (Figure 2B), except AgNPs-C1 that contain some triangle shapes. The estimation of the average NP size from TEM distribution (Figure 2C) showed that it was approximately 21, 16.5, and 6 nm for AgNPs-C1, AgNPs-C2, and AgNPs-C3, respectively, confirming the hypothesis of the lower-sized AgNPs using COSs as reducing and stabilizing agents ($p < 0.05$). Interestingly, AgNPs-C2 prepared using C2 (COS 1 h) exhibited more polydispersed NPs than those produced using C3 (COS 24 h). Such a result agrees with the UV–visible spectra given in Figure 1B, showing broad spectra with higher maximum absorbance (436 nm) than that of AgNPs-C3 (427 nm), suggesting broad AgNP distribution using C2 and lower-sized and less polydispersed AgNPs using C3. This difference in particle size distribution between two AgNPs produced using

10.3389/frfst.2024.1444298

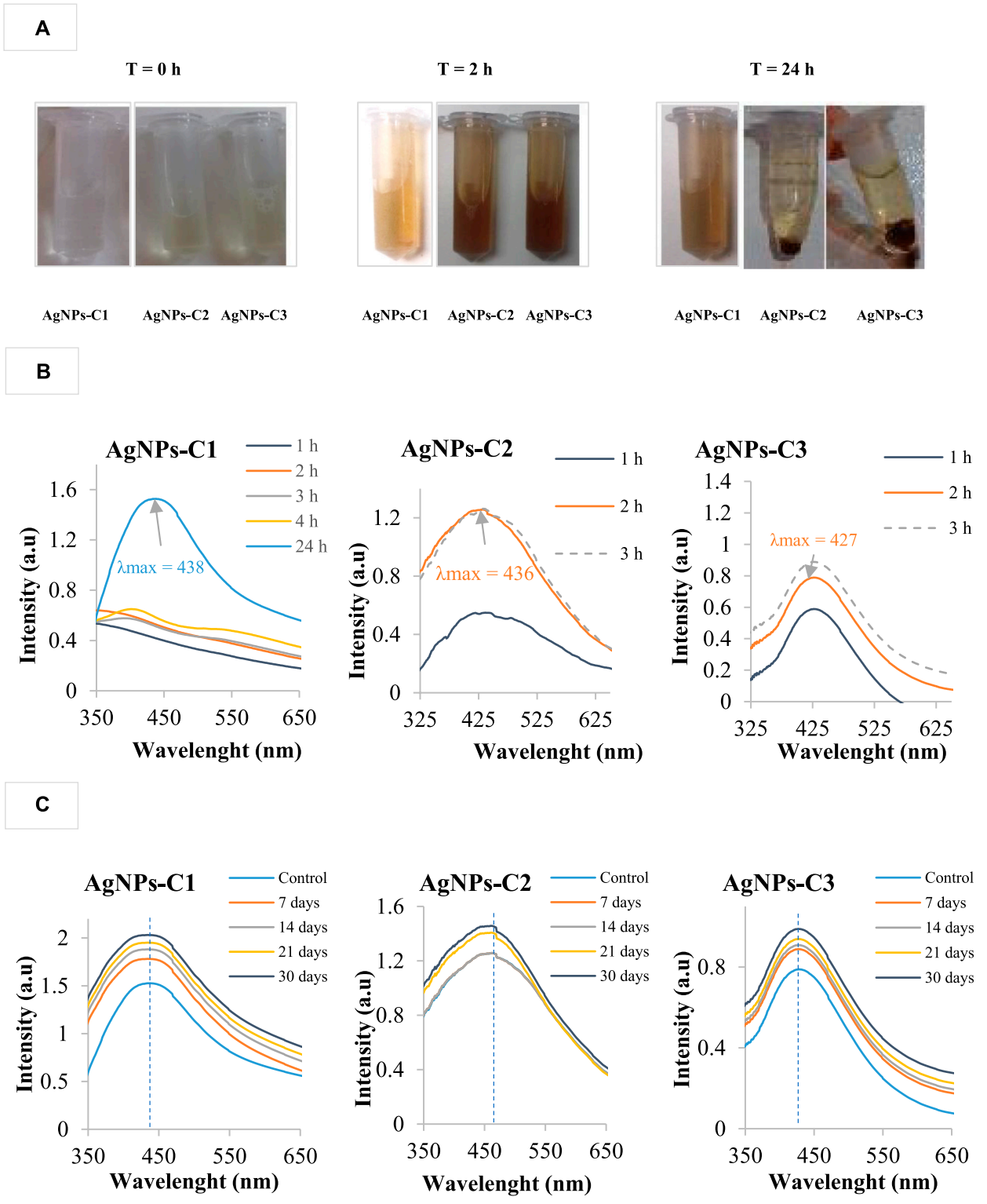

FIGURE 1
Photographs of the different silver nanoparticle solutions taken before **(1)** and after **(2)** thermal treatment for 24 h for AgNPs-C1 and 2 h for AgNPs-C2 and AgNPs-C3 **(A)**. Evolution of the UV–visible absorption spectra of silver nanoparticle synthesis using chitosan (AgNPs-C1) and chitooligosaccharides (AgNPs-C2 and AgNPs-C3) by thermal treatment at 90°C for 1, 2, 3, 4, and 24 h **(B)**. Continuous line: (–) indicates a stable solution, while not continuous line (- - -) indicates the presence of aggregates in the colloidal solution. UV–visible spectra of colloidal AgNPs during the time of storage in dark at 4°C over 7, 14, 21, and 30 days **(C)**. The control in each spectrum was the corresponding freshly prepared AgNP solution.

10.3389/frfst.2024.1444298

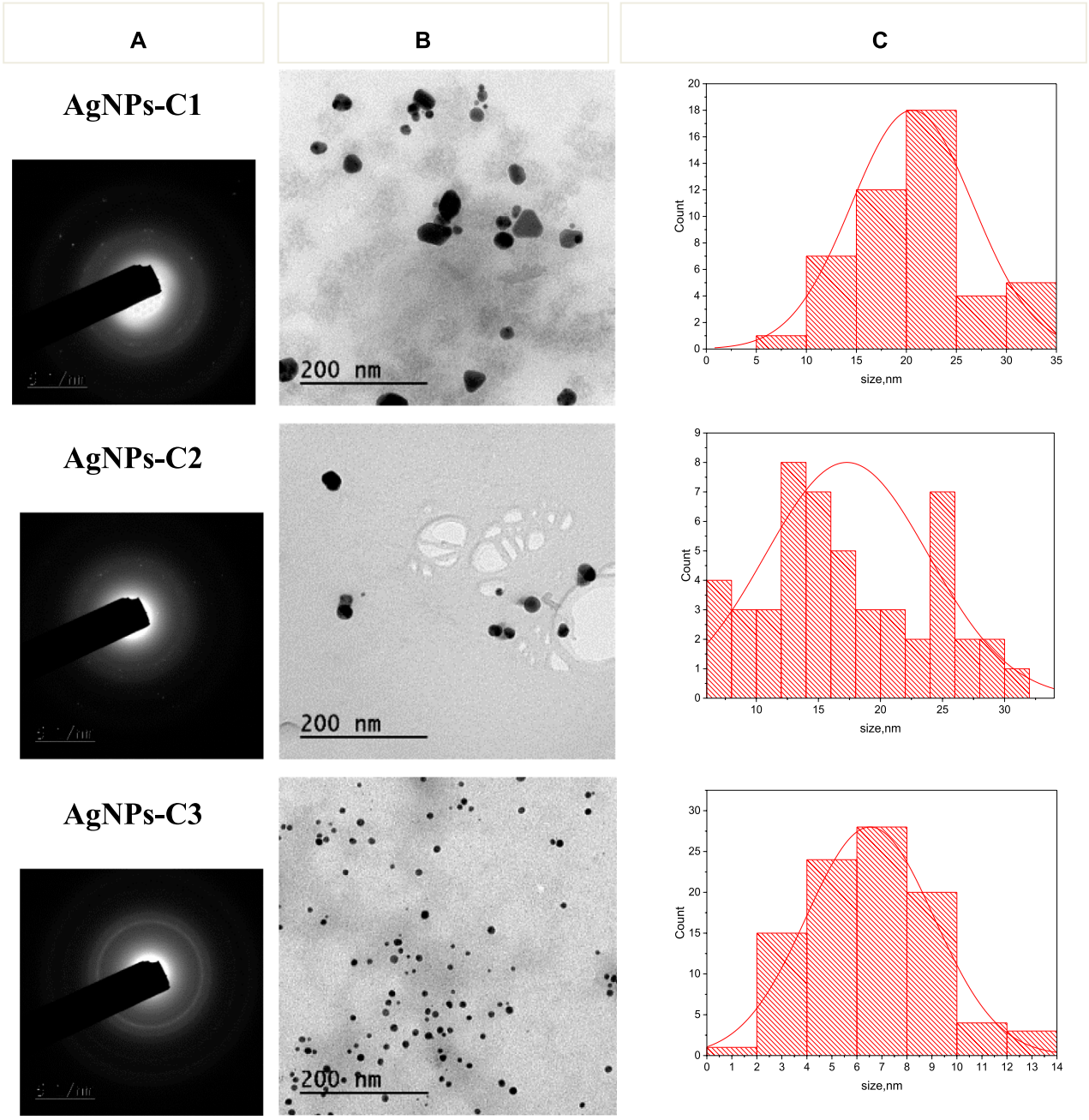

FIGURE 2
Polycrystalline nature of colloidal AgNPs based on the SAED pattern (at a magnification of ×150) **(A).** TEM micrographs of the produced colloidal AgNPs **(B)**. Particle size distribution histograms (contents in %) estimated from TEM micrographs, $n \geq 100$ **(C)**.

COS, as reducing and stabilizing agents, was probably attributed to the variation of the composition and degrees of polymerization (DP) of the used COS. Indeed, the estimation of the DP using MALDI-TOF showed that COS 2 (COS 1 h) had DP up to 17, whereas COS 3 (COS 24 h) was a mixture of hetero-chito-oligomers with DP up to 6 (Affes et al., 2019).

Similarly, the estimation of the average size of NPs using DLS analysis showed the same distribution profile, whereas DLS values were higher than those obtained by TEM. Similar micrographs were obtained by Novaes et al. (2020), who synthesized silver nanoparticles from chitosan and collagen with an average size of 25 nm by heating in the presence of $AgNO_3$ at 80°C for 2 h. In the same context, silver nanoparticles synthesized using leaf extracts of the neem plant by maceration and boiling showed particle sizes between 22 and 30 nm (Ansari et al., 2023).

The zeta potential of NPs, which is the potential that can be determined from particle mobility under an electric field, was further measured, and the results given in Table 2 show that it was found to be correlated with the Mw of chitosans and the size of NPs. Indeed, chitosan-based AgNPs showed significantly higher zeta potential (+99.3 ± 5.87 mV) than COS-based AgNPs (+23.1 ± 0.5 mV and + 16.8 ± 0.2 mV for AgNPs-C2 and AgNPs-C3,

TABLE 2 Average size (nm) and charge (mV) of AgNPs determined from TEM distribution, DLS, and zeta potential measurements.

AgNPs	Size (nm) (TEM)	Z-average (nm) (DLS)	Zeta potential (mV)
AgNPs-C1	21.0 ± 0.2^{A}	1280.05 ± 1.0^{A}	+99.3 ± 5.87^{A}
AgNPs-C2	16.5 ± 0.1^{B}	264.35 ± 0.1^{B}	+23.1 ± 0.50^{B}
AgNPs-C3	6.5 ± 0.3^{C}	141.75 ± 0.3^{C}	+16.8 ± 0.20^{B}

Values are the mean ± standard deviation (n = 3). Means with different letters (A–B) and within a column indicate significant difference ($p < 0.05$).

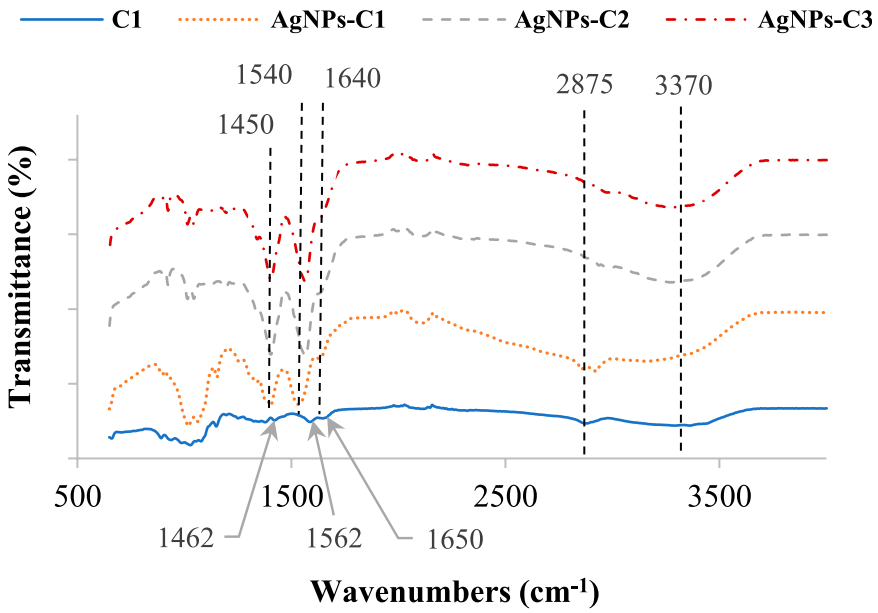

FIGURE 3
FTIR spectra of chitosan and the produced silver nanoparticles.

respectively) ($p < 0.05$). The difference in the zeta potential values might be due to the adsorption of chitosan and COS AgNPs (Dara et al., 2020; Mohan et al., 2024).

The physicochemical properties of the produced nanoparticles were studied by FTIR spectroscopy and compared to native chitosan and COS. As shown in our previous study (Affes et al., 2019), the FTIR spectra of chitosan and its derivatives were similar, with characteristic absorption bands at 3,370, 2,875, 1,650, 1,562, and 1,462 cm^{-1} attributed to the -OH, CH, amide (C=O), amine (NH) groups, and the alkyl radical -CH_2, respectively. The results given in Figure 3 reveal that in the spectra of AgNPs, the peaks observed at 1,650, 1,562, and 1,462 cm^{-1} shifted to 1,640, 1,540, and 1,450 cm^{-1}, indicating the presence of interactions between silver metal (Ag) and chitosan molecules (O and N atoms) (Hajji et al., 2017; Kalaivani et al., 2018; Dara et al., 2020; Mohan et al., 2024).

The ability of the elaborated AgNPs to produce 3D scaffolds was evaluated by a versatile freeze-drying method of the colloidal solutions. The SEM micrographs of AgNP-loaded scaffolds are given in Figure 4A and show the 3D structure achieved by freeze-drying. The results demonstrated that scaffold S1, produced using chitosan–AgNPs-C1, exhibited two different structures: (a) a uniform and porous filamentary 3D structure and (b) a smooth structure, suggesting that the nanoparticles were encapsulated into the chitosan matrix. However, SEM micrographs of the COS-based scaffolds S2 and S3 showed a smooth structure (data not shown), suggesting that COS-based AgNPs cannot produce scaffolds. The abovementioned results prove the feasibility of the chitosan–AgNP scaffold to serve as a potential biomaterial for tissue-engineering applications (Shaheen et al., 2019).

Chemical analysis of the produced scaffolds was accomplished by EDX, and an EDX spectrum of scaffold S1 is shown in Figure 4B. The results confirmed the existence of silver particles at a nanometer scale, showing a signal between 2.5 and 2.75 keV, characteristic of Ag atoms (Vinod et al., 2011).

3.2 Biological potential of the synthesized AgNPs

3.2.1 Antioxidant activity

The antioxidant activity of the elaborated AgNPs was determined and compared to chitosan and the positive control BHA using DPPH and ABTS radical-scavenging, reducing power, and total antioxidant assays. The results given in Table 3 show that all the elaborated AgNPs possessed good antioxidant potential. Furthermore, it can be concluded that this antioxidant effect was correlated with the size of AgNPs and the characteristics of the

10.3389/frfst.2024.1444298

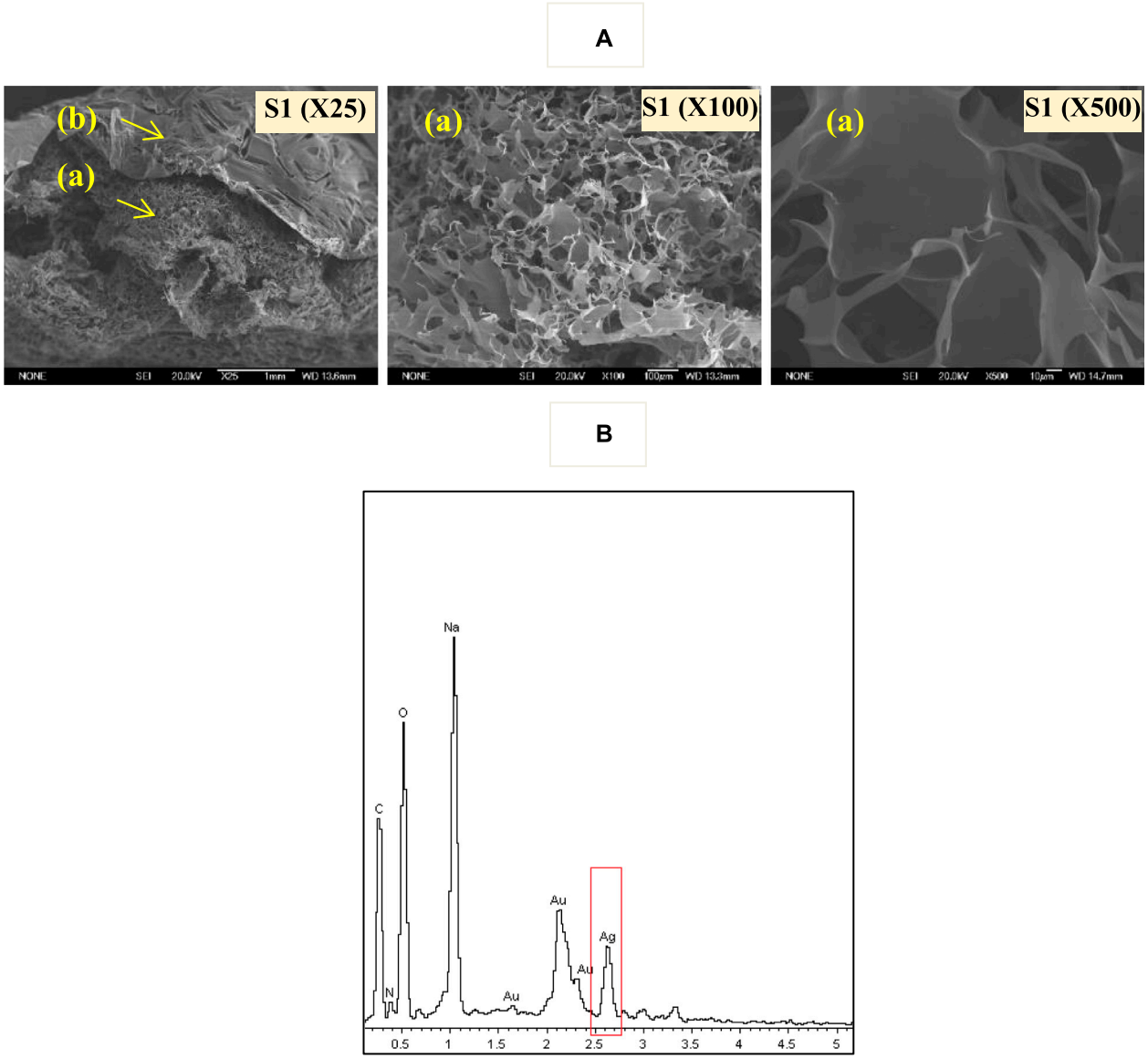

FIGURE 4
Typical SEM photo–micrographs of the synthesized AgNPs-C1 in its scaffold form (S1) **(A)**. EDX spectra of the AgNPs-C1 scaffold (S1) **(B)**.

TABLE 3 DPPH and $ABTS^{+}$ radical-scavenging activity (%), reducing power ($OD_{700\ nm}$), and total antioxidant activity (α-tocopherol [μmol/mL]) values of the elaborated silver nanoparticles compared to the positive control BHA.

Antioxidant	DPPH radical-scavenging activity (%)	$ABTS^{+}$ radical-scavenging activity (%)	Reducing power (OD_{700} nm)	Total antioxidant activity (α-tocopherol [μmol/mL])
BHA	100.00 ± 0.00^{A}	100.00 ± 0.00^{A}	3.00 ± 0.00^{A}	272.28 ± 0.04^{A}
AgNPs-C1	72.40 ± 1.10^{B}	71.60 ± 2.62^{B}	0.45 ± 0.01^{D}	95.60 ± 0.64^{D}
AgNPs-C2	100.00 ± 0.00^{A}	100.00 ± 0.00^{A}	1.37 ± 0.03^{C}	188.5 ± 1.50^{C}
AgNPs-C3	100.00 ± 0.00^{A}	100.00 ± 0.00^{A}	1.64 ± 0.01^{B}	243.00 ± 2.00^{B}

Values are the mean ± standard deviation (n = 3). Means with different letters (A–D) and within a column indicate significant difference ($p < 0.05$).

reducing and stabilizing polymer used in their preparation. Indeed, lower-sized AgNPs (AgNPs-C2 [16.5 nm] and particularly AgNPs-C3 [6.5 nm]), produced using low-Mw COS, exhibited higher antioxidant activity than AgNPs-C1 (21 nm) produced using chitosan ($p < 0.05$). For the DPPH and ABTS radical-scavenging tests, AgNPs-C2 and AgNPs-C3 exhibited very good ability to

10.3389/frfst.2024.1444298

TABLE 4 Antibacterial potential of the produced silver nanoparticles obtained through the agar well diffusion method.

Bacteria	Diameter of the inhibition zone (mm)						
	Gram (−)			Gram (+)			
	Salmonella enterica	*Pseudomonas aeruginosa*	*Enterobacter* spp.	*Staphylococcus aureus*	*Micrococcus luteus*	*Listeria monocytogenes*	*Bacillus cereus*
AgNPs-C1	16.0 ± 0.5^{B}	16.0 ± 0.2^{B}	14.5 ± 0.3^{B}	14.0 ± 0.1^{B}	14.0 ± 0.5^{B}	14.5 ± 0.4^{B}	13.0 ± 0.3^{B}
AgNPs-C2	20.0 ± 0.3^{A}	21.0 ± 0.3^{A}	19.0 ± 0.2^{A}	18.0 ± 0.5^{A}	19.0 ± 0.2^{A}	19.0 ± 0.4^{A}	16.7 ± 0.3^{A}
AgNPs-C3	16.0 ± 0.4^{B}	16.0 ± 0.3^{B}	14.0 ± 0.6^{B}	14.0 ± 0.4^{B}	14.5 ± 0.5^{B}	14.5 ± 0.4^{B}	13.5 ± 0.4^{B}

Values are the mean ± standard deviation (n = 3). Means with different superscripts (A–B) within a column indicate significant difference ($p < 0.05$).

scavenge all free DPPH and $ABTS^{+}$ radicals (100%), which is similar to the effect of BHA. Similarly, Dara et al. (2020) showed that AgNPs produced using chitosan exhibited an antioxidant potential via DPPH, FRAP, and *beta*-carotene antioxidant tests and suggested that this effect was related to the amino and hydroxyl groups of chitosan. The results revealed that the produced AgNPs may act as natural antioxidants to protect against oxidative stress related to tissue engineering, wound healing, and degenerative disease.

3.2.2 Antibacterial activity

The antibacterial potential of the produced AgNPs was assessed against three Gram (−) and four Gram (+) pathogenic bacteria using the agar well diffusion method. The results given in Table 4 reveal that the three prepared AgNPs exhibited important antibacterial effects against all tested bacteria, which differed regarding the target strain and the characteristic of AgNPs and the polymer used as the reducing and stabilizing agent in their preparation process. Indeed, the Gram (−) bacteria were significantly more inhibited than the Gram (+) strains, especially for *S. enterica* and *P. aeruginosa*, whereas the lowest effect was obtained against the Gram (+) strain *B. cereus* for all tested AgNPs. The cell wall of the Gram (+) bacteria possesses thicker peptidoglycan layers than Gram (−) strains, which prevent the uptake of Ag ions in their cytoplasm, leading to a lower antibacterial effect of AgNPs (Katas et al., 2019).

Moreover, AgNPs-C2 (16.5 nm) exhibited the significantly highest antibacterial effect against all tested bacteria, compared to AgNPs-C1 (21 nm) and AgNPs-C3 (6.5 nm) ($p < 0.05$). The latter showed the same antibacterial behavior without significant differences ($p > 0.05$). From these results, the antibacterial activity of AgNPs was related to the activity of the polymer used as the reducing and stabilizing agent in their preparation process. $COS_{1\ h}$ (C2) exhibited better antibacterial potential than chitosan and $COS_{24\ h}$ (C2), as mentioned in our previous study ($H_{24\ h}$) (Affes et al., 2019), where they are named $H_{1\ h}$ and $H_{24\ h}$, respectively. It has been reported that the antibacterial potential of AgNPs is derived from their Ag ions and their smaller sizes, which promote their diffusion through the microbial membrane, causing oxidative stress and inactivation of respiratory enzymes, important for the growth of bacterial cells, which interrupts electron transport and DNA replication and leads to bacteriolysis (Dara et al., 2020; Novaes et al., 2020; Zienkiewicz-Strzałka et al., 2020; Wu et al., 2021; Mohan et al., 2024).

4 Conclusion

Using the green method, three silver nanoparticles were produced: one using chitosan (C1) and two using chitooligosaccharides (COS: C2 and C3) as reducing and stabilizing agents, respectively. The synthesized crystalline and spherical AgNPs-C1, AgNPs-C2, and AgNPs-C3, with sizes of 21, 16.5, and 6 nm, respectively, were stable for a month at 4°C and presented excellent antioxidant and antibacterial activity, mainly COS-based AgNPs. The good biological properties elicited by AgNPs make them suitable for use as bactericidal and antioxidant agents for several biomedical and environmental applications.

Data availability statement

The raw data supporting the conclusion of this article will be made available by the authors, without undue reservation.

Author contributions

SA: conceptualization, data curation, formal analysis, investigation, methodology, resources, software, validation, visualization, writing–original draft, and writing–review and editing. IA: resources, software, writing–review and editing and supervision. NA: resources, writing–review and editing, software and supervision. ÁH: writing–review and editing, supervision. MN: resources, writing–review and editing and supervision. HM: resources, software, writing–review and editing, supervision and validation.

Funding

The author(s) declare that financial support was received for the research, authorship, and/or publication of this article. This work was funded by the Ministry of Higher Education and Scientific Research, Tunisia. The authors acknowledge financial support provided by the Spanish Ministry of Economy and Competitiveness (Grant MAT2015-65184-C2-1-R).

Conflict of interest

The authors declare that the research was conducted in the absence of any commercial or financial relationships that could be construed as a potential conflict of interest.

Publisher's note

All claims expressed in this article are solely those of the authors and do not necessarily represent those of their affiliated organizations, or those of the publisher, the editors, and the reviewers. Any product that may be evaluated in this article, or claim that may be made by its manufacturer, is not guaranteed or endorsed by the publisher.

References

Affes, S., Aranaz, I., Acosta, N., Heras, Á., Nasri, M., and Maalej, H. (2021). Chitosan derivatives-based films as pH-sensitive drug delivery systems with enhanced antioxidant and antibacterial properties. *Int. J. Biol. Macromol.* 182, 730–742. doi:10.1016/j.ijbiomac.2021.04.014

Affes, S., Aranaz, I., Hamdi, M., Acosta, N., Ghorbel-Bellaaj, O., Heras, Á., et al. (2019). Preparation of a crude chitosanase from blue crab viscera as well as its application in the production of biologically active chito-oligosaccharides from shrimp shells chitosan. *Int. J. Biol. Macromol.* 139, 558–569. doi:10.1016/j.ijbiomac.2019.07.116

Affes, S., Aranaz, I., Niuris, A., Heras, Á., Nasri, M., and Maalej, H. (2022b). Physicochemical and biological properties of chitosan derivatives with varying molecular weight produced by chemical depolymerization. *Biomass Convers. Biorefinery* 14, 4111–4121. doi:10.1007/s13399-022-02662-3

Affes, S., Maalej, H., Aranaz, I., Acosta, N., Heras, Á., and Nasri, M. (2020). Enzymatic production of low-Mw chitosan-derivatives: characterization and biological activities evaluation. *Int. J. Biol. Macromol.* 144, 279–288. doi:10.1016/j.ijbiomac.2019.12.062

Affes, S., Maalej, H., Li, S., Abdelhedi, R., Nasri, R., and Nasri, M. (2022a). Effect of glucose substitution by low-molecular weight chitosan-derivatives on functional, structural and antioxidant properties of maillard reaction-crosslinked chitosan-based films. *Food Chem.* 366, 130530. doi:10.1016/j.foodchem.2021.130530

Affes, S., Nasri, R., Li, S., Thami, T., Van Der Lee, A., Nasri, M., et al. (2020). Effect of glucose-induced Maillard reaction on physical, structural and antioxidant properties of chitosan derivatives-based films. *Carbohydr. Polym.* 255, 117341. doi:10.1016/j.carbpol.2020.117341

Ansari, M., Ahmed, S., Abbasi, A., Khan, M. T., Subhan, M., Bukhari, N. A., et al. (2023). Plant mediated fabrication of silver nanoparticles, process optimization, and impact on tomato plant. *Sci. Rep.* 13, 18048. doi:10.1038/s41598-023-45038-x

Aranaz, I., Castro, C., Heras, A., and Acosta, N. (2018). On the ability of low molecular weight chitosan enzymatically depolymerized to produce and stabilize silver nanoparticles. *Biomimetics* 3, 21. doi:10.3390/biomimetics3030021

Bersuder, P., Hole, M., and Smith, G. (1998). Antioxidants from a heated histidine-glucose model system. I: investigation of the antioxidant role of histidine and isolation of antioxidants by high-performance liquid chromatography. *J. Am. Oil Chemists' Soc.* 75, 181–187. doi:10.1007/s11746-998-0030-y

Chen, Y., Ling, Z., Mamtimin, T., Khan, A., Peng, L., Yang, J., et al. (2022). Chitooligosaccharides production from shrimp chaff in chitosanase cell surface display system. *Carbohydr. Polym.* 277, 118894. doi:10.1016/j.carbpol.2021.118894

Dara, P. K., Mahadevan, R., Digita, P. A., Visnuvinayagam, S., Kumar, L. R. G., Mathew, S., et al. (2020). Synthesis and biochemical characterization of silver nanoparticles grafted chitosan (Chi-Ag-NPs): *in vitro* studies on antioxidant and antibacterial applications. *SN Appl. Sci.* 2, 665. doi:10.1007/s42452-020-2261-y

Dong, W., Chen, Y., Xu, D., Cheng, L., Mao, L., Gao, Y., et al. (2022). Characterization and antioxidant properties of chitosan film incorporated with modified silica nanoparticles as an active food packaging. *Food Chem.* 373, 131414. doi:10.1016/j.foodchem.2021.131414

Hajji, S., Ben Slama-Ben Salem, R., Hamdi, M., Jellouli, K., Ayadi, W., Nasri, M., et al. (2017). Nanocomposite films based on chitosan-poly (vinyl alcohol) and silver nanoparticles with high antibacterial and antioxidant activities. *Process Saf. Environ. Prot.* 111, 112–121. doi:10.1016/j.psep.2017.06.018

Herrera, A., De Ávila-Montiel, G., and Polo-Corrales, L. (2018). Chitosan-based films with nanoparticles incorporated for food packaging applications. *Indian J. Sci. Technol.* 11. doi:10.17485/ijst/2018/v11i19/122783

Kalaivani, R., Maruthupandy, M., Muneeswaran, T., Hameedha Beevi, A., Anand, M., Ramakritinan, C. M., et al. (2018). Synthesis of chitosan mediated silver nanoparticles (Ag NPs) for potential antimicrobial applications. *Front. Laboratory Med.* 2, 30–35. doi:10.1016/j.flm.2018.04.002

Katas, H., Lim, C. S., Azla, A. Y. H. N., Buang, F., and Busra, M. F. M. (2019). Antibacterial activity of biosynthesized gold nanoparticles using biomolecules from *Lignosus rhinocerotis* and chitosan. *Saudi Pharm. J.* 27, 283–292. doi:10.1016/j.jsps.2018.11.010

Mohan, C. R., Kandasamy, R., and Kabiriyel, J. (2024). Correlation between electrical conductivity and antibacterial activity of chitosan-stabilized copper and silver nanoparticles. *Carbohydr. Polym. Technol. Appl.* 7, 100503. doi:10.1016/j.carpta.2024.100503

Muddin, N. A. I., Badsha, M. M., Arafath, M. A., Merican, Z. M. A., and Hossain, M. S. (2024). Magnetic chitosan nanoparticles as a potential bio-sorbent for the removal of Cr(VI) from wastewater: synthesis, envirnomental impact and challenges. *Desalination Water Treat.* 100449. In press. doi:10.1016/j.dwt.2024.100449

Novaes, J., DaSilva Filho, A. A., Bernardo, P. M., and Yapuchura, E. R. (2020). Preparation and characterization of chitosan/collagen blends containing silver nanoparticles. *Polímeros* 30, 2. doi:10.1590/0104-1428.00919

Pirtarighat, S., Ghannadnia, M., and Baghshahi, S. (2018). Green synthesis of silver nanoparticles using the plant exract of *Salvia spinosa* grown *in vitro* and their antibacterial activity assessement. *J. Nanostructure Chem.* 9, 1–9. doi:10.1007/s40097-018-0291-4

Prieto, P., Pineda, M., and Aguilar, M. (1999). Spectrophotometric quantitation of antioxidant capacity through the formation of a phosphomolybdenum complex: specific application to the determination of Vitamin E. *Anal. Biochem.* 269, 337–341. doi:10.1006/abio.1999.4019

Re, R., Pellegrini, N., Proteggente, A., Pannala, A., Yang, M., and Rice-Evans, C. (1999). Antioxidant activity applying an improved ABTS radical cation decolorization assay. *Free Radic. Biol. Med.* 26, 1231–1237. doi:10.1016/s0891-5849(98)00315-3

Reicha, F. M., Sarhan, A., Abdel-Hamid, M. I., and El-Sherbiny, I. M. (2012). Preparation of silver nanoparticles in the presence of chitosan by electrochemical method. *Carbohydr. Polym.* 89, 236–244. doi:10.1016/j.carbpol.2012.03.002

Santiago-Castillo, K., Torres-Huerta, A. M., del Ángel-López, D., Domínguez-Crespo, M. A., Dorantes-Rosales, H., Palma-Ramírez, D., et al. (2022). *In situ* growth of silver nanoparticles on chitosan matrix for the synthesis of hybrid electrospun fibers: analysis of microstructural and mechanical properties. *Polymers* 14, 674. doi:10.3390/polym14040674

Shaheen, T. I., Montaser, A. S., and Li, S. (2019). Effect of cellulose nanocrystals on scaffolds comprising chitosan, alginate and hydroxyapatite for bone tissue engineering. *Int. J. Biol. Macromol.* 121, 814–821. doi:10.1016/j.ijbiomac.2018.10.081

Tang, T. N., Nguyen, T. H. A., Tran, C. M., Doan, V. K., Nguyen, N. T. T., Vu, B. T., et al. (2023). Fabrication of silver nanoparticle-containing electrospun polycaprolactone membrane coated with chitosan oligosaccharides for skin wound car. *J. Sci. Adv. Mater. Devices* 3, 100582. doi:10.1016/j.jsamd.2023.100582

Vanden Berghe, D. A., and Vlietinck, A. J. (1991). Screening methods for antibacterial and antiviral agents from higher plants. *Methods Plant Biochem.* 6, 47–69.

Vinod, V. T. P., Saravanan, P., Sreedhar, B., Keerthi Devi, D., and Sashidhar, R. B. (2011). A facile synthesis and characterization of Ag, Au and Pt nanoparticles using a natural hydrocolloid gum kondagogu (*Cochlospermum gossypium*). *Colloids Surf. B Biointerfaces* 83, 291–298. doi:10.1016/j.colsurfb.2010.11.035

Wu, Z., Tang, S., Deng, W., Luo, J., and Wang, X. (2021). Antibacterial chitosan composite films with food-inspired carbon spheres immobilized AgNPs. *Food Chem.* 363, 130342. doi:10.1016/j.foodchem.2021.130342

Yang, D., Liu, Q., Gao, Y., Wan, S., Meng, F., Weng, W., et al. (2022). Characterization of silver nanoparticles loaded chitosan/polyvinyl alcohol antibacterial films for food packaging. *Food Hydrocoll.* 10835. In press, Journal Pre-Proof. doi:10.1016/j.foodhyd.2022.108305

Yildirim, A., Mavi, A., and Kara, A. A. (2001). Determination of antioxidant and antimicrobial activities of Rumex crispus L. extracts. *J. Agric. Food Chem.* 49, 4083–4089. doi:10.1021/jf0103572

Zienkiewicz-Strzałka, M., Deryło-Marczewska, A., Skorik, Y. A., Petrova, V. A., Choma, A., and Komaniecka, I. (2020). Silver Nanoparticles on chitosan/silica nanofibers: characterization and antibacterial activity. *Int. J. Mol. Sci.* 21, 166. doi:10.3390/ijms21010166